

# Three biofilm types produced by a model pseudomonad are differentiated by structural characteristics and fitness advantage

Anna Koza

Robyn Jerdan

Scott Cameron

Andrew J. Spiers

© A. Koza, R. Jerdan, S. Cameron, A.J. Spiers, 2020. The definitive peer reviewed, edited version of this article is published in *Microbiology*, 166(8), 2020, DOI: [10.1099/mic.0.000938](https://doi.org/10.1099/mic.0.000938)

Please, cite the final publication rather than the Authors' accepted manuscript

This manuscript is licensed under a CC-BY license  
<https://creativecommons.org/licenses/by/4.0/>



1 *Revised Manuscript with additions shown in Blue*

2 **Three biofilm-types produced by a model pseudomonad are**  
3 **differentiated by structural characteristics and fitness advantage**

4 **Anna Koza, Robyn Jerdan, Scott Cameron & Andrew J. Spiers**

5 **Affiliation:** School of Applied Sciences, Abertay University, Bell Street, Dundee DD1 1HG, UK.

6 **Author for correspondence:** Andrew J. Spiers. Email: a.spiers@abertay.ac.uk.

7 **Keywords:** Adaptive radiation, air-liquid (A-L) interface biofilms, competitive fitness, experimental  
8 evolution, microcosms, *Pseudomonas*, *P. fluorescens* SBW25, Wrinkly Spreader.

9 **Abbreviations:** A-L Interface, Air-liquid interface; CBFS, Complementary Biofilm-Forming Strain; VM,  
10 Viscous Mass; WS, Wrinkly Spreader.

11

## 12 **ABSTRACT**

13 (249 words) Model bacterial biofilm systems suggest that bacteria produce one type of biofilm which is  
14 then modified by environmental and physiological factors, though diversification of developing  
15 populations might result in the appearance of adaptive mutants producing altered structures with  
16 improved fitness advantage. Here we compare the air-liquid interface Viscous Mass (VM) biofilm  
17 produced by *Pseudomonas fluorescens* SBW25 and the Wrinkly Spreader (WS) and Complementary  
18 Biofilm-forming Strain (CBFS) biofilm-types produced by adaptive SBW25 mutants in order to better  
19 understand the link between these physical structures and the fitness advantage they provide in  
20 experimental microcosms. Wrinkly Spreader, CBFS and VM biofilms can be differentiated by strength,  
21 attachment levels and rheology, as well as by strain characteristics associated with biofilm-formation.  
22 Competitive fitness assays demonstrate that they provide similar advantage under static growth  
23 conditions but respond differently to increasing levels of physical disturbance. Pairwise competitions  
24 between biofilms suggest that these strains must be competing for at least two growth-limiting  
25 resources at the air-liquid interface, most probably O<sub>2</sub> and nutrients, though VM and CBFS cells located  
26 lower down in the liquid column might provide an additional fitness advantage through the colonisation  
27 of a less competitive zone below the biofilm. Our comparison of different SBW25 biofilm-types  
28 illustrates more generally how varied biofilm characteristics and fitness advantage could become among  
29 adaptive mutants arising from an ancestral biofilm-forming strain and raises the question of how  
30 significant these changes might be in a range of medical, biotechnological and industrial contexts where  
31 diversification and change may be problematic.

32

## 33 **INTRODUCTION**

34 Biofilms are a form of surface-associated microbial aggregation which are significant in both natural and  
35 engineered environments, impacting on colonisation and infection, competitor, predator and host  
36 interactions, community dynamics and function, *etc.* (reviewed by [1-3]). It is easy to get the impression  
37 that there is a simple dichotomy between free-living and biofilm life-styles for most bacteria, but  
38 adaptive radiation within developing biofilm populations is likely to lead to diversification unless  
39 maintained by stabilizing selection [3]. As a result, it is interesting to ask whether bacteria produce a  
40 single biofilm-type based on a linear genetic architecture involving a single sensory-regulatory system  
41 controlling one biofilm matrix or extracellular polymeric substance (EPS) biosynthesis pathway, or  
42 whether they can produce a range of different structures which better suit the environmental based on  
43 a more complex networked architecture involving multiple regulatory and biosynthesis pathways and

44 modified by adaptive mutation. This can be explored using the *Pseudomonas fluorescens* SBW25 model  
45 system in which adaptive radiation has produced a number of biofilm-types and success can be  
46 evaluated in the context of competing lineages in resource (O<sub>2</sub>)-restricted environments (reviewed by  
47 [4,5]).

48 In the SBW25 model system, the wild-type colonists of static microcosms rapidly modify their  
49 environment and differentiates the liquid column into a high-O<sub>2</sub> region at the top of the liquid column  
50 and an O<sub>2</sub>-depleted zone below [6] (this division is arbitrary; as growth continues and O<sub>2</sub> demand  
51 increases, the high-O<sub>2</sub> region becomes shallower and the O<sub>2</sub> flux deeper into the liquid column is  
52 reduced). As growth in these microcosms becomes increasingly O<sub>2</sub>-limited, the high-O<sub>2</sub> region  
53 represents an ecological opportunity [7] for any adaptive lineage capable of colonising it, as cells located  
54 here are capable of faster growth, higher final population numbers and a fitness advantage over other  
55 competitors located lower down in the liquid column (the high-O<sub>2</sub> region, which includes the A-L  
56 interface, is also referred to as the Goldilocks zone of optimal growth [8,9]; see **Supplementary Figure**  
57 **S1** for a schematic showing these regions and zones in static microcosms).

58 Adaptive lineages arise in developing or diversifying populations with key innovations that allow them to  
59 interact with their environment in a novel manner [7]. In diversifying SBW25 populations, Wrinkly  
60 Spreader (WS) mutants [10] occur with mutations affecting cyclic diguanylate (*c-di*-GMP) homeostasis  
61 and the over-production of cellulose which is the primary biofilm matrix (EPS) and a second poly-acetyl  
62 glucosamine EPS which may also acting as an attachment factor [11-15]. This results in the formation of  
63 a robust and well-attached physically cohesive-class biofilm [16] at the air-liquid (A-L) interface of static  
64 microcosms [10]. In contrast, wild-type SBW25, which does not form a biofilm under normal conditions  
65 (but see [17]), relies instead on constant aerotaxis to oppose physical disturbance and random cell  
66 diffusion, which constantly moves cells away from the high-O<sub>2</sub> region [9]. This, however, is not as  
67 effective as biofilm-formation in terms of resource utilisation and growth gains and explains why  
68 Wrinkly Spreaders often have fitness advantages over non-biofilm-forming competitors in static  
69 microcosms [10,12,18]. The underlying basis of this might be a trade-off between the use of uridine-  
70 triphosphate (UTP) for fast growth (DNA/RNA and metabolism) and the formation of uridine-  
71 diphosphate glucose (UDP-glucose) which is the precursor for cellulose [19] that enables biofilm-  
72 formation (after [20]).

73 A-L biofilm-formation is commonplace amongst environmental pseudomonads [21-25] and other  
74 bacteria, suggesting that many aerobic bacteria can gain a competitive advantage by growing in the  
75 high-O<sub>2</sub> region of static microcosms if growth is not limited by some other resource, and in several

76 model systems, including *Bacillus subtilis* 3610 [26], *P. aeruginosa* PA01 and PA14 [27,28], *P. putida*  
77 KT2440 [29] and SBW25, wild-type strains are known to produce multiple mutants with different biofilm  
78 characteristics. In addition to the Wrinkly Spreader, SBW25 produces a range of other physically  
79 cohesive-class biofilm-forming lineages with similar fitness advantage. These include the Fuzzy  
80 Spreaders evolved from wild-type SBW25 [10] which produce biofilms as the result of changes in  
81 lipopolysaccharide expression [30], and Poly-acetyl glucosamine-Wrinkly Spreader (PWS) and  
82 Complementary Biofilm-forming Strain (CBFS) mutants that evolved from a cellulose-deficient SBW25  
83 strain and over-produce poly-acetyl glucosamine [15,31]. Wild-type SBW25 can also produce a cellulose-  
84 based but fragile and poorly-attached viscous mass-class biofilm (VM) [16] when induced with  
85 exogenous Fe<sup>3+</sup> [17,32], similar to that produced by a genetically-engineered mutant using a strong  
86 promoter to over-express the cellulose biosynthesis operon [11,13]. Although these lineages arose  
87 independently from the wild-type SBW25 strain or other intermediates, they can be considered to have  
88 convergently evolved and adapted to the A-L interface of static microcosms with similar biofilms.

89 We are interested in comparing SBW25 biofilm-types, in particular the CBFS, VM and WS biofilms (see  
90 **Table 1** for key strain details including biofilm characteristics), in order to understand the link between  
91 environmental conditions, physical structure and the fitness advantage they provide. In this work, we  
92 induce wild-type SBW25 to produce VM biofilms and use a CBFS mutant as proxies for naturally-  
93 occurring SBW25 mutants which produce biofilms with similar physical characteristics and fitness  
94 advantage, and use biofilm strength and attachment measurements, rheology and other assays to  
95 quantitatively differentiate these structures and strains. We then compare CBFS, VM and WS biofilms  
96 using competitive fitness assays to determine how well suited they are to static microcosms and  
97 whether one biofilm-type is likely to be a more successful solution to the problem of colonising the A-L  
98 interface than the others.

99

## 100 **MATERIALS AND METHODS**

### 101 **Experimental microcosms, bacteria and culturing**

102 Biofilm-formation and fitness were investigated using wild-type *Pseudomonas fluorescens* SBW25  
103 [33,34] that produces the VM biofilm (to avoid confusion we refer to this as the 'VM strain' throughout),  
104 a CBFS mutant [31] and the archetypal Wrinkly Spreader (WS) mutant [11,14] (**Table 1**). SM-13 (SBW25  
105 *wssB::mini-Tn5*, selected with 50 µg ml<sup>-1</sup> kanamycin [11]), was used as a non-biofilm-forming reference  
106 strain when required. Microcosms were 30 ml universal glass vials containing 6 ml King's B liquid  
107 medium supplemented with 1 µM FeCl<sub>3</sub> required to induce the VM biofilm (KB-Fe [17]) and preliminary

108 experiments had shown that the growth and phenotypes of CBFS and WS were the same in KB-Fe as  
109 they had been reported for in KB. Inocula were obtained from shaken over-night KB-Fe cultures, and  
110 microcosms were incubated at 18-20°C statically or with increasing levels of physical disturbance  
111 provided by a Stuart SSM1 shaker operating at 30 (low level of disturbance) and 80 rpm (intermediate),  
112 and a Stuart S150 incubator operating at 150 rpm (high, i.e. vigorous shaking).

### 113 **Biofilm measurements and rheometry**

114 Biofilms were qualitatively assessed by visual inspection *in situ* and after transferring to Petri dishes  
115 [16]. Biofilm strength and attachment to the vial walls at the meniscus of static microcosms after 48 h  
116 were determined using glass balls (strength, g;  $n = 8$ ) and Crystal violet staining (attachment,  $A_{570}$ ;  $n = 8$ )  
117 [12,21]. Rheological parameters ( $G'$ ,  $G''$ ,  $G^*$ ,  $\eta_0$ , and  $\tan \delta$ ;  $n = 10 - 17$ ) of biofilm samples were measured  
118 by controlled-stress amplitude sweep tests using a MARS rotational rheometer (Thermo Scientific, UK).  
119 Measurements were made at  $20 \pm 0.1$  °C, with the storage modulus ( $G'$ ), loss modulus ( $G''$ ) and zero-  
120 point viscosity ( $\eta_0$ ) recorded. Representative data were examined graphically to determine the linear  
121 viscoelastic region of the response to the applied stress, and to find the flow point when  $G' = G''$ . The  
122 loss factor ( $\tan \delta$ ) was calculated from  $G''/G'$  and the shear modulus ( $G^*$ ) from  $\sqrt{G'^2 + G''^2}$ .

### 123 **Strain characterisation**

124 Cell-surface adhesion (nN; pooled  $n = 50$ ) was determined by Atomic force microscopy and force  
125 Spectroscopy (AFM-FS). Biofilm samples first drained of excess liquid for 30 min before being imaged in  
126 air at 20°C using a NanoWizard I Bio AFM Atomic Force microscope (JPK Instruments AG, Berlin,  
127 Germany). Samples were scanned in contact mode using silicon nitride triangular cantilevers, with a  
128 nominal spring constant of  $0.01 \text{ N m}^{-1}$ , scan speed of  $0.5 \mu\text{m s}^{-1}$  and at resolutions of  $100 \times 100 \mu\text{m}$  down  
129 to  $2.5 \times 2.5 \mu\text{m}$ . In each sample, five cells were randomly selected, and cell-tip adhesion measured at ten  
130 different points along the exposed surface of each cell. Relative cell hydrophobicity ( $H_r$ ;  $n = 5$ ) was  
131 determined using a modification of the bacterial adherence to hydrocarbons (BATH) assay [35]. 1.2 ml of  
132 culture was washed three times in PBS (pH 7.2) and the cells re-suspended to an initial optical density  
133 ( $OD_{540}$ ) of  $\sim 0.5$ . Samples were vortexed with  $300 \mu\text{l}$  of n-hexadecane for 1 min and the phases allowed  
134 to separate for 30 min. The final  $OD_{540}$  was determined for the lower aqueous phase, and  $H_r$  calculated  
135 as  $100 \times \Delta OD_{540} / \text{initial } OD_{540}$ . Maximum growth levels ( $OD_{600} 24 \text{ h}^{-1}$ ;  $n = 3$ ) were determined in shaken  
136 and static microcosms after 24 h. Liquid surface tension ( $\text{mN m}^{-1}$ ;  $n = 5$ ) was determined for cell-free  
137 culture supernatants using a Krüss K100 Tensiometer (Krüss GmbH, Germany) at 20°C [17]; under these  
138 conditions the surface tension of deionised water and sterile KB-Fe was  $72.4 \pm 0.1$  and  $49.8 \pm 0.2 \text{ mN m}^{-1}$ ,  
139 respectively. Recruitment to the surface (relative  $OD_{600}$ ;  $n = 5$ ) was measured after 2 h [13]. Cell

140 distributions (relative  $OD_{600}$ ,  $n = 5$ ) were also assessed in microcosms inoculated with a pellet of cells  
141 placed at the bottom of the vial, after 24 and 72 h, by sequentially sampling 1 ml aliquots from the top  
142 to the bottom [9]. Swimming motility (radius, cm;  $n = 3$ ) on and through soft agar (0.1x KB nutrients, 1  
143  $\mu\text{M FeCl}_3$  and 0.3 g  $\text{L}^{-1}$  agar) was assessed after 24 h. Colony expansion (radius, cm;  $n = 12$ ) on standard  
144 KB-Fe plates containing 15 g  $\text{L}^{-1}$  agar was assessed after 24 h [12].

### 145 **Competitive fitness and productivity**

146 The competitive fitness ( $W$ ) of CBFS, VM and WS were determined relative to the non-biofilm-forming  
147 SM-13 strain [18]. KB-Fe microcosms ( $n = 5$ ) were inoculated with 100  $\mu\text{l}$  of a 1:1 nominal mixture of  
148 strains (produced by adding equal volumes of over-night KB-Fe cultures) and incubated for 48 h under  
149 static or shaken conditions as required and these assays undertaken in batches for each level of  
150 disturbance. The fitness of one strain (A) competing against a second (B) was determined as the ratio of  
151 Malthusian parameters,  $\ln [A_{final} / A_{initial}] / \ln [B_{final} / B_{initial}]$  [36], and cell numbers per microcosm were  
152 determined by enumeration of colonies on KB and KB-Kanamycin plates after vigorous mixing of  
153 microcosms, sampling and serial dilution. Fitness was also determined for pair-wise combinations of  
154 biofilm-types using 1000:1, 1:1 and 1:1000 nominal initial cell ratio mixtures ( $n = 5$ ) under static  
155 incubation conditions for 72 h with all assays undertaken as a single batch. In these assays, strains  
156 differentiated by colony morphologies on KB plates, and actual strain ratios were determined from the  
157 initial cell numbers ( $A_{initial} / B_{initial}$ ). Total final numbers ( $A_{final} + B_{final}$ ) were also used to determine  
158 productivity ( $n = 5$ ) in these microcosms.

### 159 **Statistical analyses**

160 Assays were performed with replicates ( $n$ ) and means and standard errors (SE) are provided where  
161 appropriate. Data was analysed by JMP 12 (SAS Institute Inc, USA) and parametric or non-parametric  
162 approaches determined as required. Differences between means were determined using ANOVA  
163 models followed by *post hoc* Tukey-Kramer HSD tests or paired t-tests. Where appropriate the Wilcoxon  
164 (Rank Sums) tests were undertaken instead. Data were further investigated by correlation and linear  
165 regression ( $r^2$ ). See **Supplementary Information S2** for further details of the statistical approach used  
166 here and for additional analyses reported in the Supplementary Information.

167

## 168 **RESULTS AND DISCUSSION**

### 169 **CBFS, VM and WS biofilm-types are differentiable structures**

170 The three biofilm-types studied here are readily distinguished by visual observation and we have  
171 classified them as physically cohesive (CBFS and WS) and viscous mass (VM)-class biofilms [16] (**Figure 1**  
172 **(a)**). Our qualitative impressions of CBFS and WS robustness and VM fragility were confirmed by  
173 quantitative comparison of biofilm strength and attachment levels which clearly differentiates the three  
174 biofilms (T-K HSD,  $\alpha = 0.05$ ; **Figure 1 (b)** and **Table 2 (a)**). We have extended our earlier rheological  
175 examination of VM biofilm samples [17] to include CBFS and WS samples (**Table 2 (b)**). This confirms  
176 that all three were viscoelastic structures as determined by loss factors ( $\tan \delta$ ) of less than one, although  
177 other key rheological parameters differed significantly between biofilms (T-K HSD,  $\alpha = 0.05$ ; Wilcoxon,  $P$   
178  $\leq 0.05$ ; **Table 2 (b)**). Several other A-L interface biofilms, as well the VM biofilm produced by SBW25,  
179 have been examined *in situ* by interfacial rheology which also conclude that these are viscoelastic  
180 structures [37,38] as is the case for the more often studied liquid-solid surface (L-S) interface biofilms in  
181 which cells are similarly encased by a network of EPS fibres [39]. We interpret our results to suggest that  
182 the WS biofilm is the more resilient structure and is less brittle than the CBFS biofilm, and that both are  
183 stronger and better attached than the fragile VM biofilm.

184 Biofilm-formation also depends on a number of strain characteristics. These include swimming (and  
185 twitching) motility, relative cell hydrophobicity and cell adhesion, and the expression of surface active  
186 agents which are needed to approach, modify and successfully colonise a surface or interface. We  
187 observed significant differences in swimming in soft agar, with CBFS and WS cells apparently retarded by  
188 the over-expression of poly-acetyl glucosamine (CBFS), and cellulose and poly-acetyl glucosamine (WS),  
189 compared to VM cells (T-K HSD,  $\alpha = 0.05$ ; **Table 2 (c)**) which presumably produce lower levels of these  
190 EPS or are not expressing them under these conditions. However, CBFS and VM cells swam at similar  
191 rates on the surface of soft agar which suggests the CBFS phenotype might change, perhaps in response  
192 to surface viscosity, other factors or interactions (the percentage of agar used in these assays is too low  
193 for swarming, although SBW25 is capable of this surface-associated motility [40]). Significant  
194 differences were also observed in recruitment rates to the top of the liquid column, relative cell  
195 hydrophobicity, and cell-surface adhesion, as well as in colony expansion which had previously been  
196 used to characterise the WS phenotype [12,41,42] (T-K HSD,  $\alpha = 0.05$ ; **Table 2 (c)**) (we know that  
197 recruitment and adhesion of SBW25 and mutant cells are affected by EPS expression [9,13,43], and  
198 other studies suggest that large amounts of EPS may promote cell adhesion, e.g. [44]; a similar range of  
199 cell hydrophobicities are seen for other pseudomonads, e.g. [45], though  $H_r$  varies with the hydrocarbon  
200 tested [46]). However, no significant differences were seen in the surface tension of culture  
201 supernatants suggesting that all three expressed the surfactant viscosin [47], or in growth rates which  
202 suggests that they responded to  $O_2$  levels in the same manner (T-K HSD,  $\alpha = 0.05$ ; **Table 2 (c)**). However,  
203 it is notable that, across all three strains, a 1.4x higher growth level was achieved in shaken microcosms



204 with higher levels of aeration than static microcosms with more limited O<sub>2</sub> access (paired t-test,  $P <$   
205 0.0001).

206 Thirteen of 15 quantitative measurements we have made of biofilm strength and attachment levels,  
207 biofilm rheology and strain characteristics (**Table 2**) differentiate between CBFS, VM and WS biofilms.  
208 More similarities were found between CBFS and VM biofilms than with the WS biofilm, as determined  
209 by HCA (**Supplementary Figure S2**), which differs from our early qualitative grouping of these biofilms  
210 into physically cohesive and viscous mass-class biofilms [16] (**Figure 1 (a)**). Nonetheless, both the  
211 qualitative and quantitative assessments of biofilm phenotypes demonstrate that the CBFS, VM and WS  
212 biofilms can be differentiated by a number of characteristics and can be considered substantially  
213 different structures (quantitative biofilm phenotypes have not been reported for collections of WS or  
214 CBFS-like mutant isolates, e.g. in [10,14,15,48,49], so the range and overlap of biofilm-type phenotypes  
215 is unknown).

216 Our findings add to the growing number of reports demonstrating that naturally-occurring and  
217 engineered mutants are able to alter the physical characteristics of the biofilms produced by the wild-  
218 type strain, including KT2440, PA01 and PA14 which produce adaptive mutants similar to the Wrinkly  
219 Spreader in diversifying populations [27,28,29]. It would be interesting to know whether the variation in  
220 biofilm characteristics between wild-type and mutant strains is similar to the variation between wild-  
221 type biofilms grown under a range of environmental conditions, as this would impact on the fitness  
222 advantage biofilm mutants may have in diversifying populations and their ability to colonise new  
223 environments. Finally, as we have no reason to suppose that CBFS and VM-like biofilm mutants could  
224 not arise directly from wild-type SBW25 in one or two mutations, our physical comparison of these  
225 three proxy biofilm-types illustrates how adaptive radiation could result in multiple biofilm-based  
226 solutions to colonising the high-O<sub>2</sub> region of liquid columns through parallel or convergent evolution  
227 [50] (our use of the CBFS partially-engineered mutant and manipulation of wild-type SBW25 with  
228 exogenous Fe<sup>3+</sup> were required as natural mutants with CBFS and VM biofilm phenotypes were not  
229 available).

### 230 **Competitive fitness depends on the degree of physical disturbance**

231 Although increased access to O<sub>2</sub> at the A-L interface underlies the fitness advantage of biofilm formation  
232 [5], these structures need to be sufficiently robust to withstand random physical disturbance yet still be  
233 cost-effective in terms of resource allocation for biofilm construction and growth. We therefore predict  
234 that as disturbance is increased, fitness should decline to the point where biofilm-formation provides no  
235 advantage or incurs a cost compared to non-biofilm-forming competitors. We tested competitive

236 fitness at four levels of disturbance, from standard static incubation conditions where disturbance is  
237 rare, low and intermediate levels of disturbance provided by a smooth-running orbital shaker, to high  
238 levels of disturbance provided by a more vigorous shaking incubator. Under low disturbance conditions,  
239 48 h old CBFS and WS biofilms remained at the A-L interface but the VM biofilm sank within an hour,  
240 and under intermediate levels of disturbance all three biofilms sank within an hour.

241 Under static conditions the CBFS biofilm was found to provide the highest level of competitive fitness  
242 compared to the non-biofilm-forming reference strain SM-13 (W for CBFS,  $2.7 \pm 0.1$ ) and significant  
243 differences in fitness were seen between all three strains (W for VM,  $2.2 \pm 0.1$ ; WS,  $1.8 \pm 0.1$ ; T-K HSD,  $\alpha$   
244 = 0.05). Furthermore, under these conditions each of the biofilm-forming strains can be considered  
245 adaptive lineages as fitness was greater than one (t-tests,  $P < 0.05$ ), in agreement with earlier studies of  
246 VM and WS biofilms [11,32], and therefore are examples of convergent evolution (some prefer the term  
247 parallel evolution [48] but see [50]) (fitness or selection coefficients within WS and CBFS-like mutant  
248 isolates is known to vary e.g. [14,15,30,48,49], but as experimental conditions and reference strains  
249 differ, we cannot comment on the overlap of fitness ranges between biofilm-types). Our fitness assays  
250 also demonstrate that competitive fitness significantly declines with increasing levels of physical  
251 disturbance (T-K HSD,  $\alpha = 0.05$ ) (**Figure 2**) (in contrast, total productivity increases with disturbance, in  
252 agreement with our understanding that growth is  $O_2$ -limited in these microcosms; see **Supplementary**  
253 **Figure S3**). CBFS fitness fell the most, though only WS fitness was reduced to below one in the most  
254 vigorous shaking conditions (t-test,  $P = 0.006$ ) (see **Supplementary Information S3** for further analysis of  
255 the fitness data confirming strain and disturbance effects).

256 These results clearly demonstrate that CBFS, VM and WS biofilm-forming lineages can out-compete a  
257 non-biofilm-forming competitor in static microcosms, but that as physical disturbance increases, the  
258 adaptive value of biofilm-formation rapidly falls in a strain and disturbance-dependent manner. In  
259 particular, we note that WS fitness did not change between static and low disturbance conditions,  
260 whereas CBFS and VM fitness significantly decreased (T-K HSD,  $\alpha = 0.05$ ) (**Figure 2**), supporting our  
261 earlier view that the WS biofilm was the more resilient structure and the VM biofilm the most fragile.  
262 We therefore conclude that the WS biofilm is better suited to the range of physical disturbance static  
263 microcosms are normally subject to than either the CBFS or VM biofilms.

#### 264 **Pair-wise competitions between CBFS, VM and WS**

265 We undertook pair-wise competitive fitness assays with initial cell ratios of 1:1000, 1:1 and 1000:1 to  
266 determine which biofilm-former was likely to be successful if two mutants appeared at the same time in  
267 a radiating population, or if a second mutant appeared sometime after the first had become established

268 (three-way assays with two biofilm-forming strains plus SM-13 pose too many technical difficulties to  
269 be considered here). In these assays, both competitors are mixed uniformly throughout the liquid  
270 column and cells have to move into the high-O<sub>2</sub> region before they can form biofilms (similar assays  
271 have been undertaken before to determine relative fitness or selection coefficients within biofilm-types,  
272 e.g. [14,30,48,49]).

273 At or near the initial cell ratio of 1:1, the competitive fitness of CBFS and VM was significantly greater  
274 than WS fitness (**Figure 3**; T-K HSD,  $\alpha = 0.05$ ), suggesting that these two strains can more rapidly  
275 colonise and dominate the A-L interface by forming biofilms than the WS under the conditions used  
276 here. However, across the range of initial cell ratios tested in these assays, fitness was found to be  
277 negative-frequency dependent for all pair-wise combinations and ranged between  $0.52 \pm 0.03$  and  $1.9 \pm$   
278  $0.1$  for WS competing against VM when dominant and VM competing against WS when rare,  
279 respectively (**Figure 3**; a linear fit was found between the fitness of each strain and the log initial cell  
280 ratio,  $r^2 = 0.77 - 0.98$ ; and fitness was also negatively correlated within strain pairs,  $r^2 = -0.96 - -0.98$ ,  $P <$   
281  $0.0001$ ) (see **Supplementary Information S4** for further analysis of the fitness data confirming strain and  
282 ratio effects, and **Supplementary Figure S4** and **Supplementary Information S5** for an analysis of  
283 productivity that also confirms strain effects). We interpret these findings to mean that the fitness of  
284 CBFS, VM and WS biofilms is determined by strain characteristics and relative numbers, and to a lesser  
285 extent, on the identity of the competitor.

286 Negative frequency-dependent fitness arises as the proportions of competing strains change and within-  
287 strain competition for at least one limiting resource becomes more important than between-strain  
288 competition for the same resource (the suggestion that the increasing mass of the WS biofilm and  
289 likelihood of it sinking explains WS fitness decrease [3] does not apply to our model system, as in our  
290 two-day assays biofilms rarely sank). However, the reciprocal nature of the fitness within our pairwise  
291 biofilm competitions suggest that two limiting resources are needed to differentiate between the three  
292 strains. Although this will require further investigation, we suspect they are O<sub>2</sub> and nutrients; the  
293 presence of an extreme O<sub>2</sub> gradient within WS biofilms has already been established [6] and it is  
294 possible that a similar but inverted nutrient gradient is limiting growth at the very top layer of the  
295 biofilm (when nutrient levels are sufficiently low, O<sub>2</sub> is no longer growth-limiting and the WS fitness  
296 advantage is lost [8]; it would be intriguing to investigate cell distributions and fitness in microcosms  
297 containing nitrate or nitrite as alternative terminal electron acceptors, though we do not know whether  
298 SBW25 is capable of using these in anaerobic respiration). In the context of our model system, it is  
299 possible that multiple biofilm types may appear and co-exist for various lengths of time within the  
300 biofilm structure, where cell surface properties and EPS retain growing clonal populations and displace

301 competitors and diversity is maintained by multiple limiting resources allowing metabolic and growth  
302 trade-offs [2,3], even though the ready recognition of WS colonies on plates suggests that this is the  
303 most abundant and successful biofilm-type.

304 As substantial growth appears to occur in the liquid column below the VM biofilm compared to CBFS  
305 and WS biofilms (**Figure 1 (a)**), it is possible that some of the VM fitness advantage might be due to the  
306 colonisation of this region, as fitness is determined from total microcosm numbers rather than numbers  
307 from the biofilm itself. We confirmed that CBFS, VM and WS cell localisation throughout the liquid  
308 column varied with depth (T-K HSD,  $\alpha = 0.05$ ; **Figure 4 (a-c)**) and between the three strains, with CBFS  
309 and WS having a higher proportion at the top than VM (Relative OD<sub>600</sub> after 24 h, CBFS,  $3.87 \pm 0.11$ ; WS,  
310  $3.55 \pm 0.06$ ; VM,  $1.89 \pm 0.03$ ; T-K HSD,  $\alpha = 0.05$ ; **Figure 4 (d)**) (enrichment at the top of the liquid column  
311 requires aerotaxis which has been demonstrated for both wild-type SBW25 and WS cells [9]). It is  
312 interesting to note that although the proportion of VM cells at the top did not significantly increase  
313 between 24 h and 72 hr, the proportion of WS cells increased (1.2x) as the WS biofilm became more  
314 visually obvious and the proportion of CBFS cells decreased (0.8x) as the liquid column below the CBFS  
315 biofilm became more turbid (T-K HSD,  $\alpha = 0.05$ ; **Figure 4 (d)**). The proportion of VM cells located in the  
316 middle of the liquid column was significantly higher than CBFS and the proportion of WS cells the lowest  
317 (Relative OD<sub>600</sub> after 24 h, CBFS,  $0.60 \pm 0.02$ ; WS,  $0.39 \pm 0.02$ ; VM,  $0.78 \pm 0.02$ ; T-K HSD,  $\alpha = 0.05$ ; **Figure**  
318 **4 (e)**; see **Supplementary Information S6** for an analysis of cell distributions confirming strain and depth  
319 effects). These differences in cell localisation may reflect how CBFS, VM and WS biofilm structures  
320 develop over time and how efficiently each is able to retain their growing populations. However,  
321 localisation at the top does not require biofilm-formation per se, as wild-type SBW25 cells inhibited  
322 from forming a VM biofilm are also able to enrich in this region, though not as effectively as WS cells [9].  
323 Nonetheless, the ability to colonise both the A-L interface by biofilm-formation and the rest of the liquid  
324 column with free-swimming cells might also reflect might reflect a trade-off between growth and  
325 competition, with cells near the A-L interface growing fast but subject to high levels of competition, and  
326 cells located further down the liquid column growing more slowly but with less competition.

327

## 328 CONCLUSIONS

329 Although biofilm research now has many established model systems, SBW25 is one of only a few  
330 bacteria reported to form a variety of A-L interface biofilms produced by adaptive mutants arising in  
331 diversifying populations or by genetic engineering. Our work has shown that the CBFS, VM and WS  
332 biofilms can be differentiated on the basis of physical structure, strain characteristics and fitness

333 advantage, allowing a link to be made between environmental conditions in which biofilms form, the  
334 structural resilience these must have in order to survive, and the fitness advantage they provide over  
335 other competitors. Although we have used the CBFS and VM biofilms here as proxies for naturally-  
336 occurring adaptive mutants which might arise in diversifying SBW25 populations as the Wrinkly  
337 Spreader did, our comparison of the three biofilm-types also illustrates how varied biofilm  
338 characteristics and fitness advantage might become between adaptive mutants arising from an  
339 ancestral biofilm-forming strain. It is possible that this variation may be greater than that seen between  
340 biofilms produced by the ancestor under different environmental conditions, and both variation in  
341 biofilm characteristics and the fitness advantage they provide may have significance in a range of  
342 medical, biotechnological and industrial contexts where the success of prophylactic treatments or  
343 continued productivity could be effected by unexpected diversity or change.

344

#### 345 **SUPPORTING INFORMATION AND DATA**

346 Supporting information is available as a Supplementary Information file. *This will be made available*  
347 *from Mendeley Data on acceptance.*

#### 348 **AUTHOR STATEMENTS**

349 ORCID Author identifiers: Robyn Jerdan, 0000-0002-7045-8362; Andrew Spiers, 0000-0003-0463-8629.  
350 Roles undertaken by the Authors: Anna Koza: Design, experimentation and analysis; Robyn Jerdan:  
351 Design, experimentation, analysis and manuscript development; Scott Cameron: Manuscript  
352 development and supervision; Andrew Spiers: Design, experimentation, analysis, manuscript  
353 development and supervision. All authors contributed to the final manuscript preparation.

#### 354 **CONFLICTS OF INTERESTS**

355 The authors declare that there are no conflicts of interests.

#### 356 **FUNDING INFORMATION**

357 This work was partially funded by Abertay University (Scottish Charity Registration No: SC016040). Anna  
358 Koza's PhD studentship was funded by Abertay University while Robyn Jerdan's PhD studentship is self-  
359 funded.

360 **ACKNOWLEDGMENTS**

361 We thank Robert Jackson (University of Reading) and David Studholme (University of Exeter) for the  
362 sequencing of the CBFS2.1 genome, Paul Hallett (now at the University of Aberdeen) for help with the  
363 rheometry and Simon Hapca (now at the University of Stirling) for help with the initial statistical  
364 analyses. Andrew Spiers is a member of the Scottish Alliance for Geoscience Environment and Society  
365 (SAGES) and Anna Koza was a SAGES-associated PhD student.

366

367 **REFERENCES**

- 368 [1] **Flemming H-C, Wingender J, Szewzyk U, Steinberg P, Rice SA, Kjelleberg S.** Biofilms: an emergent  
369 form of bacterial life. *Nat Rev Microbiol* 2016;14:563–575.
- 370 [2] **Nadell CD, Drescher K, Foster KR.** Spatial structure, cooperation and competition in biofilms. *Nat*  
371 *Rev Microbiol* 2016;14:589–600.
- 372 [3] **Steenackers HP, Parijs I, Foster KR, Vanderleyden J.** Experimental evolution in biofilm  
373 populations. *FEMS Microbiol Rev* 2016;40:373–397.
- 374 [4] **Spiers AJ.** A mechanistic explanation linking adaptive mutation, niche change, and fitness  
375 advantage for the Wrinkly Spreader. *Int J Evolutionary Biol* 2014; Article ID 675432.
- 376 [5] **Koza A, Kuśmierska A, McLaughlin K, Moshynets O, Spiers AJ.** Adaptive radiation of  
377 *Pseudomonas fluorescens* SBW25 in experimental microcosms provides an understanding of the  
378 evolutionary ecology and molecular biology of A-L interface biofilm formation. *FEMS Microbiol*  
379 *Lett* 2017;364:fnx109.
- 380 [6] **Koza A, Moshynets O, Otten W, Spiers AJ.** Environmental modification and niche construction:  
381 developing O<sub>2</sub> gradients drive the evolution of the Wrinkly Spreader. *ISME J* 2011;5:665–673.
- 382 [7] **Yoder JB, Clancey E, Des Roches S, Eastman JM, Gentry L, Godsoe W, Hagey TJ, Jochimsen D,**  
383 **Oswald BP, Roberston J, Sarver BAJ, Schenks JJ, Spear SF, Harmon LJ.** Ecological opportunity and  
384 the origin of adaptive radiations. *J Evolutionary Biol* 2010;23:1581-1596.
- 385 [8] **Kuśmierska A, Spiers AJ.** New insights into the effects of several environmental parameters on  
386 the relative fitness of a numerically dominant class of evolved niche specialist. *Int J Evolutionary*  
387 *Biol* 2016;4846565.

- 388 [9] **Jerdan R, Kuśmierska A, Petric M, Spiers AJ.** Penetrating the air-liquid interface is the key to  
389 colonization and Wrinkly Spreader fitness. *Microbiology* 2019;165:1061–1074.
- 390 [10] **Rainey PB, Travisano T.** Adaptive radiation in a heterogeneous environment. *Nature*  
391 1998;394:69–72.
- 392 [11] **Spiers AJ, Kahn SG, Travisano M, Bohannon J, Rainey PB.** Adaptive divergence in experimental  
393 populations of *Pseudomonas fluorescens*. I. Genetic and phenotypic bases of Wrinkly Spreader  
394 fitness. *Genetics* 2002;161:33–46.
- 395 [12] **Spiers AJ, Bohannon J, Gehrig S, Rainey PB.** Biofilm formation at the air–liquid interface by the  
396 *Pseudomonas fluorescens* SBW25 wrinkly spreader requires an acetylated form of cellulose. *Mol*  
397 *Microbiol* 2003;50:15–27.
- 398 [13] **Spiers AJ, Rainey PB.** The *Pseudomonas fluorescens* SBW25 wrinkly spreader biofilm requires  
399 attachment factor, cellulose fibre and LPS interactions to maintain strength and integrity.  
400 *Microbiology* 2005;151:2829–2839.
- 401 [14] **Bantinaki B, Kassen R, Knight CG, Robinson Z, Spiers AJ, Rainey PB.** Adaptive divergence in  
402 experimental populations of *Pseudomonas fluorescens*. III. Mutational origins of Wrinkly Spreader  
403 diversity. *Genetics* 2007;176:441–453.
- 404 [15] **Lind PA, Farr AD, Rainey PB.** Evolutionary convergence in experimental *Pseudomonas*  
405 populations. *ISME J* 2017;11:589–600.
- 406 [16] **Spiers AJ, Arnold DL, Moon CD, Timms-Wilson TM.** A survey of A-L biofilm formation and  
407 cellulose expression amongst soil and plant-associated *Pseudomonas* isolates. In: *Microbial*  
408 *Ecology of Aerial Plant Surfaces*. Bailey MJ, Lilley AK, Timms-Wilson TM (Eds). Wallingford: CABI;  
409 2006. pp. 121–132.
- 410 [17] **Koza A, Hallett PD, Moon CD, Spiers AJ, 2009.** Characterisation of a novel air–liquid interface  
411 biofilm of *Pseudomonas fluorescens* SBW25. *Microbiology* 2009;155:1397–1406.
- 412 [18] **Green JH, Koza A, Moshynets O, Pajor R, Ritchie M., Spiers AJ.** Evolution in a test tube: rise of the  
413 Wrinkly Spreaders. *J Biological Educ* 2011;45:54–59.
- 414 [19] **Römling U, Galperin MY.** Bacterial cellulose biosynthesis: diversity of operons, subunits, products,  
415 and functions. *Trends Microbiol* 2015;23:545–557.

- 416 [20] **Remigi P, Ferguson GC, McConnell E, De Monte S, Rogers DW, Rainey PB.** Ribosome provisioning  
417 activates a bistable switch coupled to fast exit from stationary phase. *Mol Biol Evol* 2019;36:1056–  
418 1070.
- 419 [21] **Ude S, Arnold DL, Moon CD, Timms-Wilson T, Spiers AJ.** Biofilm formation and cellulose  
420 expression among diverse environmental *Pseudomonas* isolates. *Environ Microbiol* 2006;8:1997–  
421 2011.
- 422 [22] **Gjermansen M, Ragas P, Tolker-Nielsen T.** Proteins with GGDEF and EAL domains regulate  
423 *Pseudomonas putida* biofilm formation and dispersal. *FEMS Microbiol Lett* 2006;265:215–224.
- 424 [23] **Nielsen L, Li X, Halverson LJ.** Cell–cell and cell–surface interactions mediated by cellulose and a  
425 novel exopolysaccharide contribute to *Pseudomonas putida* biofilm formation and fitness under  
426 water-limiting conditions. *Environ Microbiol* 2011;13:1342–1356.
- 427 [24] **Robertson M, Hapca SM, Moshynets O, Spiers AJ.** Air-liquid interface biofilm formation by  
428 psychrotrophic pseudomonads recovered from spoiled meat. *Antonie van Leeuwenhoek*  
429 2013;103:251–259.
- 430 [25] **Farias GA, Olmedilla A, Gallegos M-T.** Visualization and characterization of *Pseudomonas*  
431 *syringae* pv. tomato DC3000 pellicles. *Microbial Biotechnol* 2019;0:1–15.
- 432 [26] **Dragos A, Lakshmanan N, Martin M, Horvaath B, Maroti G, Garcia CF, Lieleg O, Kovacs AT.**  
433 Evolution of exploitative interactions during diversification in *Bacillus subtilis* biofilms. *FEMS*  
434 *Microbiol Ecol* 2018;94:fix155.
- 435 [27] **Boles BR, Thoendel M, Singh PK.** Self-generated diversity produces “insurance effects” in biofilm  
436 communities. *PNAS (USA)* 2004;101:16630–16635.
- 437 [28] **Flynn KM, Dowell G, Johnson TM, Koestler BJ, Waters CM, Cooper VS.** Evolution of ecological  
438 Diversity in Biofilms of *Pseudomonas aeruginosa* by altered cyclic diguanylate signalling. *J*  
439 *Bacteriol* 2016;198:2608–2618.
- 440 [29] **Bridier A, Piard JC, Bouchez T.** Emergence of a synergistic diversity as a Response to Competition  
441 in *Pseudomonas putida* biofilms. *Microb Ecol* 2019; 10.1007/s00248-019-01470-z.
- 442 [30] **Ferguson GC, Bertels F, Rainey PB.** Adaptive divergence in experimental populations of  
443 *Pseudomonas fluorescens*. V. Insight into the niche specialist Fuzzy Spreader compels revision of  
444 the model *Pseudomonas* radiation. *Genetics* 2013;195:1319–1335.



- 445 [31] **Gehrig SM.** Adaptation of *Pseudomonas fluorescens* SBW25 to the air-liquid interface: a study in  
446 evolutionary genetics. DPhil Thesis. Oxford: University of Oxford; 2005.
- 447 [32] **Koza A.** Adaptation and niche construction by *Pseudomonas fluorescens* SBW25. DPhil Thesis.  
448 Dundee: Abertay University; 2011.
- 449 [33] **Bailey MJ, Thompson IP.** Detection systems for phyllosphere Pseudomonads. In: *Genetic*  
450 *Interactions Between Microorganisms in the Natural Environment*. Wellington EMR, van Elsas JD  
451 (Eds). Oxford: Pergamon Press; 1992. pp. 127–141.
- 452 [34] **Rainey PB, Bailey MJ.** Physical and genetic map of the *Pseudomonas fluorescens* SBW25  
453 chromosome. *Mol Microbiol* 1996;19:521–533.
- 454 [35] **Rosenberg M.** Bacterial adherence to hydrocarbons: a useful technique for studying cell surface  
455 hydrophobicity. *FEMS Microbiol Lett* 1984;22:289-295.
- 456 [36] **Lenski RE, Rose M., Simpson SC, Tadler SC.** Long-term experimental evolution in *Escherichia coli*.  
457 I. Adaptation and divergence during 2,000 generations. *Amer Nat* 1991;138:1315–1341.
- 458 [37] **Wu C, Lim JY, Fuller GG, Cegelski L.** Quantitative analysis of amyloid-integrated biofilms formed  
459 by uropathogenic *Escherichia coli* at the air-liquid interface. *Biophys J* 2012;103:464-471.
- 460 [38] **Rühs PA, Böni L, Fuller GG, Inglis RF, Fischer P.** In-situ quantification of the interfacial rheological  
461 response of bacterial biofilms to environmental stimuli. *PLoS ONE* 2013;8:e78524.
- 462 [39] **Peterson BW, He Y, Ren Y, Zerdoum A, Libera MR, Sharma PK, Van Winkelhoff A-J, Neut D,**  
463 **Stoodleu P, Van der Mei H, Busscher HJ.** Viscoelasticity of biofilms and their recalcitrance to  
464 mechanical and chemical challenges. *FEMS Microbiol Rev* 2015;39:234–245.
- 465 [40] **Alsohim AS, Taylor TB, Barrett GA, Gallie J, Zhang X-X, Altamirano-Junqueira AE, Johnson LJ,**  
466 **Rainey PB, Jackson RW.** The biosurfactant viscosin produced by *Pseudomonas fluorescens* SBW25  
467 aids spreading motility and plant growth promotion. *Environ Microbiol* 2014;16:2267–2281.
- 468 [41] **Spiers AJ.** Wrinkly-Spreader fitness in the two-dimensional agar plate microcosm: maladaptation,  
469 compensation and ecological success. *PLoS ONE* 2007;2:e740.
- 470 [42] **Udall YC, Deeni Y, Hapca SM, Raikes D, Spiers AJ.** The evolution of biofilm-forming Wrinkly  
471 Spreaders in static microcosms and drip-fed columns selects for subtle differences in wrinkleality  
472 and fitness. *FEMS Microbiol Ecol* 2015;91:fiv057.

- 473 [43] **Fang HHP, Chan K-Y, Xu L-C.** Quantification of bacterial adhesion forces using atomic force  
474 microscopy (AFM). *J Microbiological Meth* 2000;40:89–97.
- 475 [44] **Tsuneda S, Aikawa H, Hayashi H, Yuasa A, Hirate A.** Extracellular polymeric substances  
476 responsible for bacterial adhesion onto solid surface. *FEMS Microbiol Lett* 2003;223:287–292.
- 477 [45] **Vanhaecke E, Remon J-P, Moors M, Raes F, De Rudder D, Van Peteghem A.** Kinetics of  
478 *Pseudomonas aeruginosa* adhesion to 304 and 316-L stainless steel: role of cell surface  
479 hydrophobicity. *Appl Envir Microbiol* 1990;56:788–795.
- 480 [46] **Stoimenova E, Vasileva-Tonkova E, Sotirova A, Galabova D, Lalchev Z.** Evaluation of different  
481 carbon sources for growth and biosurfactant production by *Pseudomonas fluorescens* isolated  
482 from wastewaters. *Z Naturforsch* 2009;64c:96–102.
- 483 [47] **de Bruijn I, de Kock MJ, Yang M, de Waard P, van Beek TA, Raaijmakers JM.** Genome-based  
484 discovery, structure prediction and functional analysis of cyclic lipopeptide antibiotics in  
485 *Pseudomonas* species. *Mol Microbiol* 2007;63:417–428.
- 486 [48] **McDonald MJ, Gehrig SM, Meintjes PL, Zhang X-X, Rainey PB.** Adaptive divergence in  
487 experimental populations of *Pseudomonas fluorescens*. IV. Genetic constraints guide evolutionary  
488 trajectories in a parallel adaptive radiation. *Genetics* 2009;183:1041–1053.
- 489 [49] **Lind PA, Farr AD, Rainey PB.** Experimental evolution reveals hidden diversity in evolutionary  
490 pathways. *eLife* 2015;4:e07074.
- 491 [50] **Arendt J, Reznick D.** Convergence and parallelism reconsidered: what have we learned about the  
492 genetics of adaptation? *Trends Ecol Evol* 2008;23:26–32.

493

494

## 495 **FIGURE LEGENDS**

496

497 **Figure 1. The three biofilms produced by SBW25 have different phenotypes.** Shown here are images of  
498 biofilms in situ and ex situ (a). Wild-type SBW25 (Ctrl) normally grows throughout the liquid column of  
499 static microcosms and does not produce a biofilm at the A-L interface or lumps of material when  
500 transferred to a Petri dish. In contrast, the CBFS and WS biofilms are robust-looking structures with a  
501 dry-looking top surface, are well-attached to the vial walls and produce large fragments when

502 transferred. The VM biofilm is a weak and poorly attached structure with a very wet-looking top surface  
503 and produces viscous strands of material when transferred. The control culture was grown in standard  
504 KB media and the CBFS, VM and WS biofilms in KB-Fe media. Microcosms were incubated for 72 h  
505 before testing. The three biofilms can be further differentiated by quantitative measurements of biofilm  
506 strength (g) and attachment levels ( $A_{570}$ ) (**b**). Microcosms were incubated for 48 h before assay and  
507 means  $\pm$  SE ( $n = 8$ ) are shown. Means not connected by the same letter (normal text, strength; italics,  
508 attachment) are significantly different (T-K HSD,  $\alpha = 0.05$ ).

509 **Figure 2. The fitness advantage of biofilm–formation is reduced as physical disturbance increases.**

510 Shown are the competitive fitness ( $W$ ) of CBFS, VM and WS (**a – c**) relative to the non-biofilm–forming  
511 reference strain SM-13 in microcosms incubated with increasing degrees of physical disturbance  
512 (indicated by the triangles at the bottom of each graph), ranging from static (1) to vigorous shaking (4)  
513 conditions. When  $W > 1$  the biofilm–forming strain has a competitive advantage over SM-13; when  $W <$   
514 1 SM-13 has the advantage. Microcosms were inoculated with a 1:1 ratio of the biofilm-forming strain  
515 and SM-13 and were incubated for 48 h before assay. Means  $\pm$  SE ( $n = 5$ ) are shown. Means not  
516 connected by the same letter within panels are significantly different (T-K HSD,  $\alpha = 0.05$ ). The grey  
517 background indicates  $W < 1$ . Dashed lines indicate trends only. Fitness under shaking conditions were  
518 further tested and means marked with an asterisk indicate where  $W \neq 1$  (t-test,  $P \leq 0.05$ ).

519 **Figure 3. Pairwise competitions between CBFS, VM and WS biofilms in static microcosms.** Shown are  
520 the competitive fitness ( $W$ ) of CBFS, VM and WS relative to one another in static microcosms inoculated  
521 with different initial strain ratios (**a – c**). When  $W > 1$  the first strain has a competitive advantage over  
522 the second strain; when  $W < 1$  the second strain has the advantage over the first strain. The small  
523 triangles indicate at what log ratio the strains are neutral (i.e.  $W = 1$ ). Microcosms were inoculated with  
524 nominal 1:1000, 1:1 and 1:1000 cell ratios of the first and second strains, but data are shown here using  
525 the actual ratios determined from the initial cell number colony counts. Microcosms were incubated for  
526 72 h before assay. Means  $\pm$  SE ( $n = 5$ ) are shown. Means not connected by the same letter within panels  
527 are significantly different (T-K HSD,  $\alpha = 0.05$ ). The grey background indicates  $W < 1$ . Dashed lines  
528 indicate trends only.

529 **Figure 4. Cells distributions vary through the liquid column.** Shown are the cell densities (relative  
530  $OD_{600}$ ) in samples (1 – 6) taken serially down the liquid column of static microcosms (**a – c**, CBFS, VM and  
531 WS), from the top and including any biofilm material (1) to the bottom (6). Cell densities in the top and  
532 middle samples (2 – 5) are compared on the right (**d & e**). Microcosms were inoculated with a cell pellet  
533 placed at the bottom of the vial and then incubated for 24 h (white circles) or 72 h (grey circles) before

534 assay. Means  $\pm$  SE ( $n = 5$ ) are shown. Means not connected by the same letter within panels are  
535 significantly different (T-K HSD,  $\alpha = 0.05$ ). The grey background indicates where relative densities are  
536 below one. Dashed lines indicate trends only.

537

538

539 **TABLES**540 **Table 1 : Biofilm-types produced by wild-type *P. fluorescens* SBW25 and mutants.**

541	Complementary		
542	Biofilm-forming Strain (CBFS)	Viscous Mass (VM)	Wrinkly Spreader (WS)
543	<hr/>		
544	<b>Strain origin</b>	Diversifying population of	Wild-type strain
545		the cellulose-deficient	
546		SBW25 <i>wssΔ</i> mutant	Diversifying population of
547			wild-type SBW25
548	<b>Genotype</b>	SBW25 <i>wssΔ awsX</i> (CBFS2.1 [31]) <sup>a</sup>	SBW25 (wild-type [33,34])
549			SBW25 <i>wspF</i> (archetypal strain
550			[11,14])
551	<b>Biofilm induction</b>	Genetic ( <i>awsX</i> ),	Physiological,
552		elevated <i>c-di</i> -GMP levels <sup>b</sup>	exogenous Fe <sup>3+</sup>
553			Genetic ( <i>wspF</i> ),
554	<b>Biofilm characteristics</b>	Physically cohesive-class biofilm <sup>c</sup>	Viscous mass-class biofilm <sup>c</sup>
555		Robust and well attached	Fragile and poorly attached
556		Dry-looking upper surface	Wet-looking upper surface
557			Physically cohesive-class biofilm <sup>c</sup>
558	<b>Biofilm matrix / EPS</b>	PGA <sup>b</sup>	Small amounts of cellulose, PGA
559			Higher levels of cellulose, PGA
560	<b>Liquid column</b>	Relatively little growth	More growth evident growth
561			Relatively little growth
562	<b>Colony morphology</b>	Intermediate, rough but	Smooth and rounded
563		rounded	Flattened and wrinkled
564	<hr/>		

565 **a**, See **Supplementary Information S1** for our identification of the likely biofilm-activating mutation in *awsX*. **b**, After similar  
566 mutants in which *c-di*-GMP and PGA were implicated by genetic means [15]. **c**, According to the classification of [16].

567

568

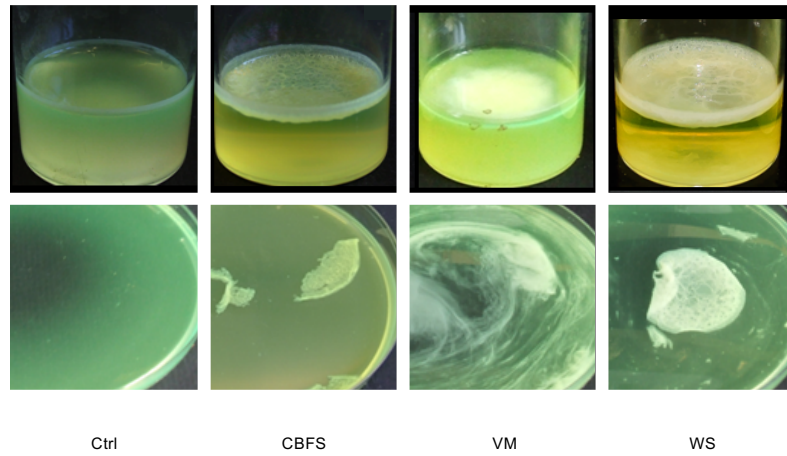
569

570 **Table 2 : Quantitative differentiation of CBFS, VM and WS biofilms and strains.**

571		CBFS	VM	WS
572				
573	<b>(a) Biofilm measurements</b>			
	Attachment ( $A_{570}$ )	1.79 ± 0.03 <sup>a</sup>	0.12 ± 0.01 <sup>c</sup>	0.27 ± 0.02 <sup>b</sup>
574	Strength (g)	0.030 ± 0.002 <sup>b</sup>	0.009 ± 0.003 <sup>c</sup>	0.208 ± 0.005 <sup>a</sup>
575				
576	<b>(b) Biofilm rheometry</b>			
	Flow point ( $G' = G''$ ) (Pa)	0.014 ± 0.001 <sup>*</sup>	0.028 ± 0.004 <sup>*</sup>	14 ± 2 <sup>*</sup>
577	Loss factor ( $\tan \delta$ )	0.52 ± 0.02 <sup>a</sup>	0.46 ± 0.01 <sup>a</sup>	0.28 ± 0.02 <sup>b</sup>
578	Shear modulus <sup>†</sup> ( $G^*$ ) (Pa)	0.27 ± 0.02 <sup>*</sup>	0.8 ± 0.2 <sup>*</sup>	130 ± 36 <sup>*</sup>
579	Zero shear viscosity ( $\eta_0$ ) (Pa s)	0.087 ± 0.005 <sup>*</sup>	0.24 ± 0.05 <sup>*</sup>	41 ± 11 <sup>*</sup>
580				
581	<b>(c) Strain characteristics</b>			
	Cell hydrophobicity ( $H_t$ )	0.44 ± 0.02 <sup>a</sup>	0.19 ± 0.02 <sup>b</sup>	0.08 ± 0.03 <sup>c</sup>
582	Cell-surface adhesion (nN)	-13.2 ± 0.1 <sup>b</sup>	-12.1 ± 0.1 <sup>a</sup>	-15.2 ± 0.2 <sup>c</sup>
583	Colony expansion (cm 24 h <sup>-1</sup> )	0.38 ± 0.01 <sup>b</sup>	0.40 ± 0.01 <sup>b</sup>	0.75 ± 0.02 <sup>a</sup>
584	Growth in shaken microcosms (OD <sub>600</sub> 24 h <sup>-1</sup> )	1.39 ± 0.04 <sup>a</sup>	1.38 ± 0.02 <sup>a</sup>	1.38 ± 0.03 <sup>a</sup>
585	Growth in static microcosms (OD <sub>600</sub> 24 h <sup>-1</sup> )	1.00 ± 0.01 <sup>ab</sup>	1.01 ± 0.03 <sup>a</sup>	0.91 ± 0.02 <sup>b</sup>
586	Liquid surface tension (mN m <sup>-1</sup> )	25.6 ± 0.2 <sup>a</sup>	25.2 ± 0.2 <sup>a</sup>	25.8 ± 0.1 <sup>a</sup>
587	Recruitment (relative OD <sub>600</sub> )	0.70 ± 0.02 <sup>b</sup>	0.77 ± 0.01 <sup>a</sup>	0.80 ± 0.02 <sup>a</sup>
588	Swimming in soft agar (cm 24 h <sup>-1</sup> )	0.28 ± 0.03 <sup>b</sup>	0.93 ± 0.07 <sup>a</sup>	0.35 ± 0.08 <sup>b</sup>
589	Swimming on soft agar (cm 24 h <sup>-1</sup> )	1.2 ± 0.05 <sup>a</sup>	1.08 ± 0.08 <sup>a</sup>	0.53 ± 0.06 <sup>b</sup>

591 Means ± SE are shown. Means not connected by the same letter are significantly different (T-K HSD,  $\alpha = 0.05$ ), and where  
592 appropriate, \* indicates where all pairwise combinations are significantly different (Wilcoxon,  $P \leq 0.05$ ). †, Also known as the  
593 modulus of rigidity and sometimes denoted by S or  $\mu$ . Biofilm rheometry for the VM biofilm was originally presented in [17].

(a) Biofilms *in situ* and *ex situ*



(b) Biofilm strength and attachment

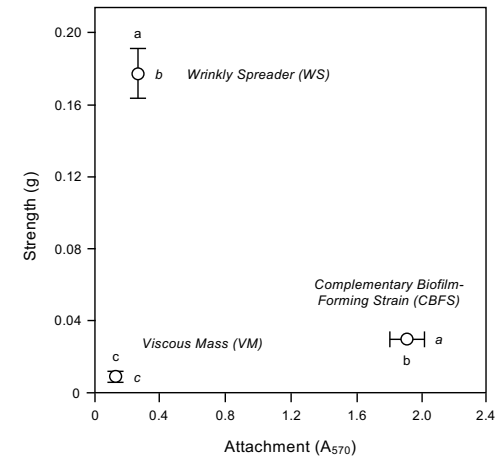


Figure 1

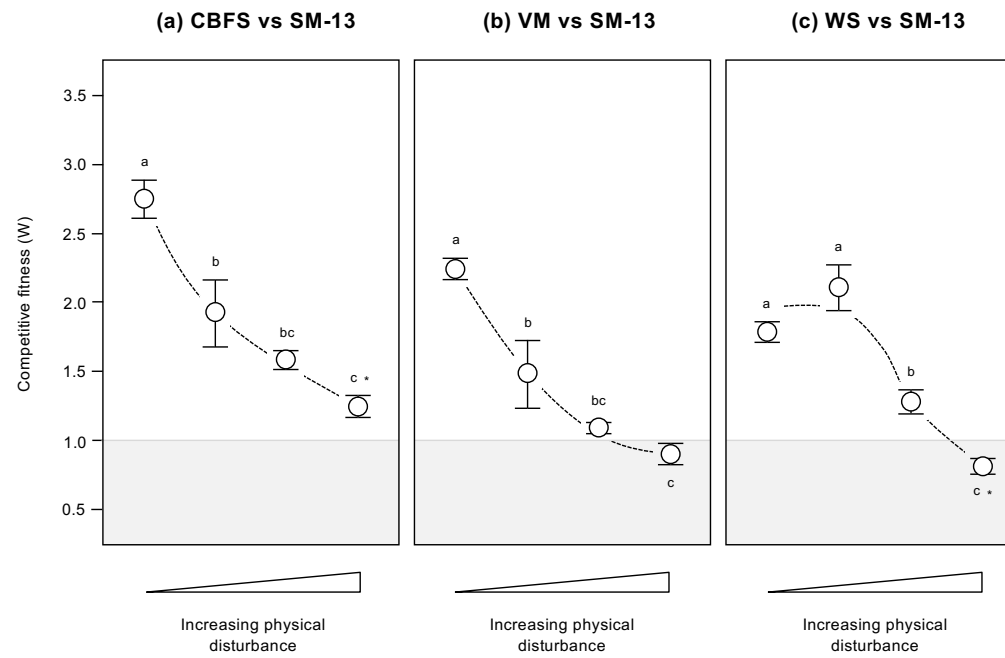


Figure 2



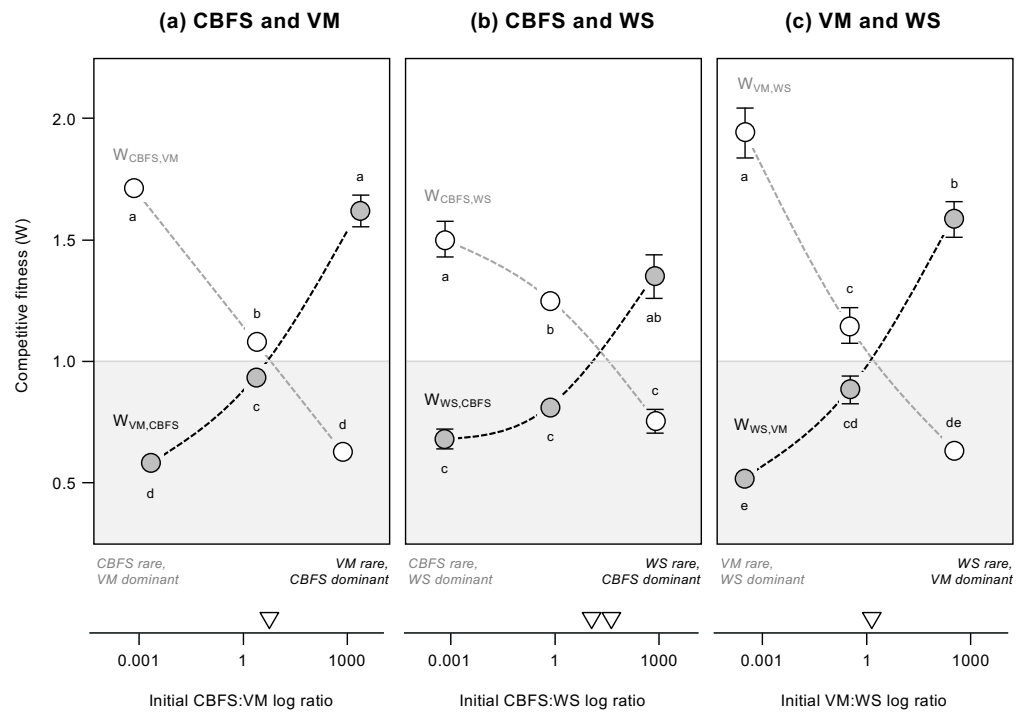


Figure 3



## SUPPLEMENTARY INFORMATION

# Three biofilm types produced by a model pseudomonad are differentiated by structural characteristics and fitness advantage

Anna Koza, Robyn Jerdan, Scott Cameron, and Andrew J. Spiers

## SUPPLEMENTARY INFORMATION SECTIONS S1 – S6

### S1: Identification of the *awsX* mutation in CBFS2.1

CBFS2.1 was an unknown biofilm-forming mutant isolated from a diversifying population of the cellulose-deficient SBW25 strain, SBW25  $\Delta wss$  [1]. We determined the genome sequence of CBFS2.1 with the help of Robert Jackson (University of Reading) and David Studholme (University of Exeter) in which a mutation in *awsX* (PFLU5211) was identified involving the deletion of 11 amino acids (YTDDLKIGTTQ). *AwsX* is a regulator of the diguanylate cyclase (DGC) *AwsR*, and mutations in *awsX* in a wild-type SBW25 background result in the WS phenotype [2] through increased *c-di*-GMP levels and activation of the cellulose synthase complex. However, *awsX* mutations in a SBW25  $\Delta wss$  background result in the over-expression of PGA instead (these are collectively known as the PWS mutants [3]). For this reason, we suggest that CBFS2.1 is similar to the PWS mutants and also expresses PGA to produce an A-L interface biofilm.

#### S1 References

- [1] **Gehrig SM.** Adaptation of *Pseudomonas fluorescens* SBW25 to the air-liquid interface: a study in evolutionary genetics. DPhil Thesis. Oxford: University of Oxford; 2005..
- [2] **McDonald MJ, Gehrig SM, Meintjes PL, Zhang X-X, Rainey PB.** Adaptive divergence in experimental populations of *Pseudomonas fluorescens*. IV. Genetic constraints guide evolutionary trajectories in a parallel adaptive radiation. *Genetics* 2009;183:1041–1053.
- [3] **Lind PA, Farr AD, Rainey PB.** Evolutionary convergence in experimental *Pseudomonas* populations. *ISME J* 2017;11:589–600.

### S2: Statistical analyses

Assays were performed with replicates ( $n$ ) as a single batch unless otherwise indicated and means and standard errors (SE) are provided where appropriate. Data was analysed by JMP 12 (SAS Institute Inc, USA) using a parametric approach having first determined that the data or residuals had a Normal distribution. Where necessary, outlier analysis was used and data progressively removed until a Normal distribution was achieved, as determined by fitting a Normal distribution and using the Shapiro-Wilk W Test ( $P > 0.05$ ) to check the goodness of fit. Differences between means were determined using ANOVA models followed by *post hoc* Tukey-Kramer HSD tests. Where necessary, a nonparametric comparison using the Wilcoxon method was employed instead. A paired t-test was used to investigate differences in growth in shaken and static microcosms, and further t-tests used to determine if competitive fitness was equal to one. Similarities between biofilms was investigated by Hierarchical cluster analysis (HCA) using the Ward method with ordinal values derived from the biofilm structure, rheology and strain characterisation data. General linear (mixed) modelling (GLM/GLMM with Summary of fit, RSquare) approaches with standard least squares personalities were used to model competitive fitness and productivity with *post hoc* differences between means determined using LSMeans Differences Student's t and Tukey HSD tests. Correlations between data were examined ( $r^2$ ) and fits between fitness as the response and log [initial cell ratio] as the regressor were determined by linear regression.

### **S3: Further analysis of competitive fitness across a range of physical disturbance levels**

Competitive fitness was modelled using a GLM approach with strain (CBFS, VM, WS; character, nominal), disturbance (four levels from static (1) to shaken (4); character, ordinal) and replicate (character, nominal) effects, and a strain x disturbance interaction effect (GLM summary statistics: RSquare = 0.89; ANOVA,  $F_{15,40} = 21.85$ ,  $P < 0.0001$ ). This found significant strain, disturbance and strain x disturbance interaction effects ( $P < 0.0001$ ,  $P < 0.0001$  and  $0.0003$ ), but no replicate effect ( $P = 0.53$ ). Both strain and disturbance levels could be further differentiated, with CBFS having the highest over-all fitness of 1.85 across the range of disturbances, followed by WS (1.45) and then VM (1.41), and the static incubation conditions producing the highest fitness of 2.24 across the strains and the shaking incubation producing the lowest fitness of 0.97 as expected (LSMeans Differences T-HSD,  $\alpha = 0.05$ ).

### **S4: Further analysis of competitive fitness from the pairwise competitions**

Competitive fitness was first modelled using a GLMM approach for each pairwise competition, with first strain (CBFS, VM, WS; character, nominal), ratio (log of the actual initial cell ratio, calculated for the first strain) (numeric, continuous), and replicate effects and a first strain x ratio interaction effect. In the CBFS and VM competitions (GLMM summary statistics: RSquare = 0.98; ANOVA,  $F_{7,17} = 150.03$ ,  $P < 0.0001$ ), first strain, ratio and first strain x ratio interaction effects ( $P < 0.0001$ ,  $0.02$  and  $< 0.0001$ ) were found, but no replicate effect ( $P = 0.96$ ). However, no significant correlation was found between the pooled fitness and log ratio ( $P = 0.41$ ). In the CBFS and WS competitions (GLMM summary statistics: RSquare = 0.88; ANOVA,  $F_{7,21} = 21.11$ ,  $P < 0.0001$ ), significant first strain and first strain x ratio interaction effects ( $P < 0.0001$ ) were found, but no ratio or replicate effects ( $P = 0.19$  and  $0.99$ ). No correlation was found between the pooled fitness and log ratio ( $P = 0.5$ ). Finally, in the VM and WS competitions (GLMM summary statistics: RSquare = 0.97; ANOVA,  $F_{7,15} = 65.88$ ,  $P < 0.0001$ ), significant first strain and first strain x ratio interaction ( $P = 0.004$  and  $< 0.0001$ ) effects and a weak ratio effect ( $P = 0.06$ ) were found, but no replicate effect ( $P = 0.48$ ). However, no significant correlation was found between the pooled fitness and log ratio ( $P = 0.75$ ). In all three models, both strains could be differentiated from one another (LSMeans Differences Student's  $t$ ,  $\alpha = 0.05$ ). These confirm that strain fitness is differentiated within pairwise assays, and that fitness is dependent on the initial cell ratios.

Competitive fitness was also modelled using a GLMM approach for all pairwise competitions, with first strain, strain pair (CBFS & VM, CBFS & WS, VM & WS; character, nominal), ratio and replicate (character, nominal) effects (GLMM summary statistics: RSquare = 0.91; ANOVA,  $F_{9,67} = 74.96$ ,  $P < 0.0001$ ). This found significant first strain, strain pair and ratio effects ( $P < 0.0001$ ,  $0.005$  and  $0.0001$ ) effects, but no replicate effect ( $P = 0.95$ ). However, no significant correlation was found between the pooled fitness and log ratio ( $P = 0.49$ ). This confirms the effect findings from the individual models and in addition shows that there are significant differences in fitness between each of the strain combinations tested in these pairwise assays.

### **S5: Further analysis of productivity from the pairwise competitions**

Productivity was modelled using a GLMM approach with strains (CBFS & VM, CBFS & WS, VM & WS; character, nominal), ratio (log of the actual initial cell ratio, calculated for the first strain) (numeric, continuous), and replicate effects (GLMM summary statistics: RSquare = 0.36; ANOVA,  $F_{7,37} = 2.96$ ,  $P = 0.01$ ). This found a significant strain effect ( $P = 0.003$ ) and a weak ratio effect ( $P = 0.07$ ), but no replicate effect ( $0.78$ ). A weak correlation was also found between the pooled productivity and log ratio ( $r^2 = 0.30$   $P = 0.4$ ). This confirms that productivity is affected by the strain combinations and initial cell ratios.

### **S6: Further analysis of cell distributions**

Cell distributions were modelled using a GLM approach separately for the 24 and 72 h incubation experiments as a Normal distribution of residuals was not readily achieved for the combined data. For both experiments, cell distributions were modelled with strain (CBFS, VM, WS, character, nominal), depth (1 – 6, numeric, ordinal) and replicate (character, nominal)

effects (GLM summary statistics for the 24 h experiment: RSquare = 0.99; ANOVA,  $F_{11,64} = 491.51$ ,  $P < 0.0001$ ; 48 h experiment: RSquare = 0.99; ANOVA,  $F_{11,56} = 413.81$ ,  $P < 0.0001$ ). This found significant strain and depth effects (24 and 72 h,  $P < 0.0001$ ) but no replicate effects (24 h,  $P = 0.24$ ; 72 h,  $P = 0.40$ ). In both experiments, CBFS, VM and WS could be differentiated from one another (LSMeans Differences T-HSD,  $\alpha = 0.05$ ), and the top (1), middle-depth samples (2 – 5) and bottom (6) samples from one another (LSMeans Differences T-HSD,  $\alpha = 0.05$ ).

## SUPPLEMENTARY INFORMATION FIGURES S1 – S4

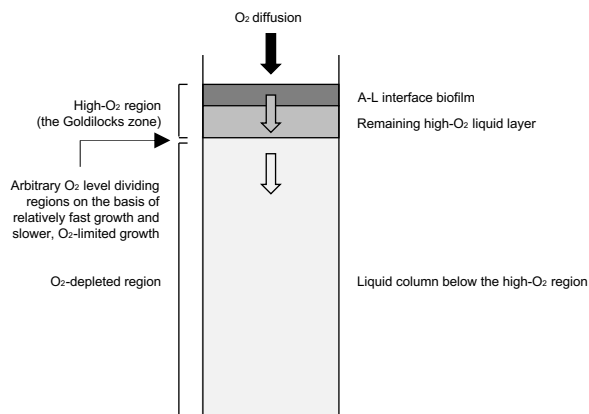


**Figure S1. The static microcosm is divided into different regions.** The metabolic activity of the initial SBW25 colonists randomly distributed through the liquid column rapidly establishes an O<sub>2</sub> gradient and divides the microcosm into a shallow high-O<sub>2</sub> region and a deeper O<sub>2</sub>-depleted region. An air-liquid (A-L) interface biofilm can be formed at the liquid surface of the high-O<sub>2</sub> region, and both this and the remaining high-O<sub>2</sub> layer below it are also known as the Goldilocks zone. However, as the biofilm develops and deepens, O<sub>2</sub> flux through the biofilm is further reduced and the high-O<sub>2</sub> liquid layer becomes shallower (ultimately the division between high-O<sub>2</sub> and depleted-O<sub>2</sub> regions moves up into the biofilm).

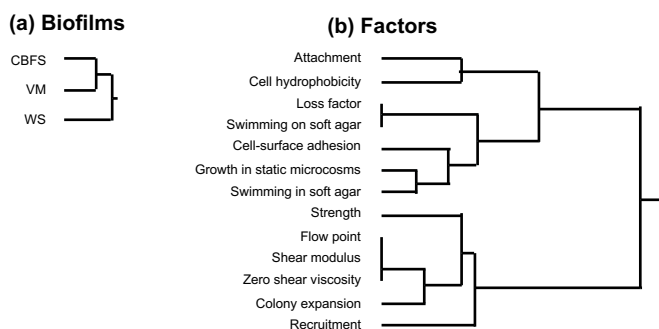


**Figure S2. Biofilms are differentiated by a range of quantifiable factors.** Shown are the results of a two-way Hierarchical cluster analysis (HCA) using biofilm structure, rheology and strain characterisation data ( $n = 13$ ). Biofilms are clustered according to similarity in (a) and factors according to similarity in (b).

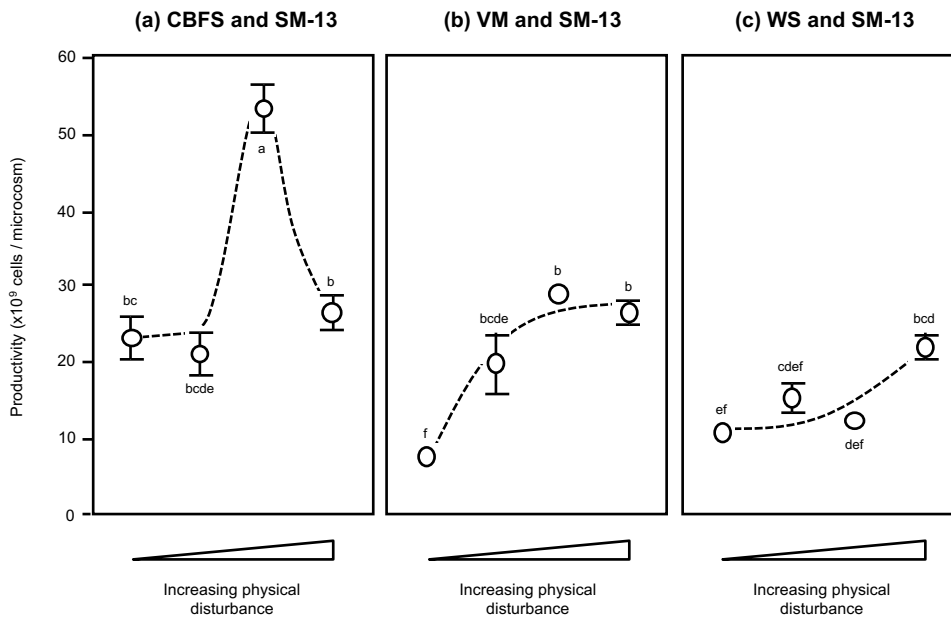


**Figure S3. Productivity in the physical disturbance assays.** Shown are the productivities determined as the total final cell numbers (a – c, CBFS, VM or WS plus SM-13) per microcosm for the competitive fitness assays which were incubated with increasing degrees of physical disturbance (indicated by the triangles at the bottom of each graph), ranging from static (1) to vigorous shaking (4) conditions. Means  $\pm$  SE ( $n = 5$ ) are shown. Means not connected by the same letter within and across panels are significantly different (T-K HSD,  $\alpha = 0.05$ ). Dashed lines indicate trends only.

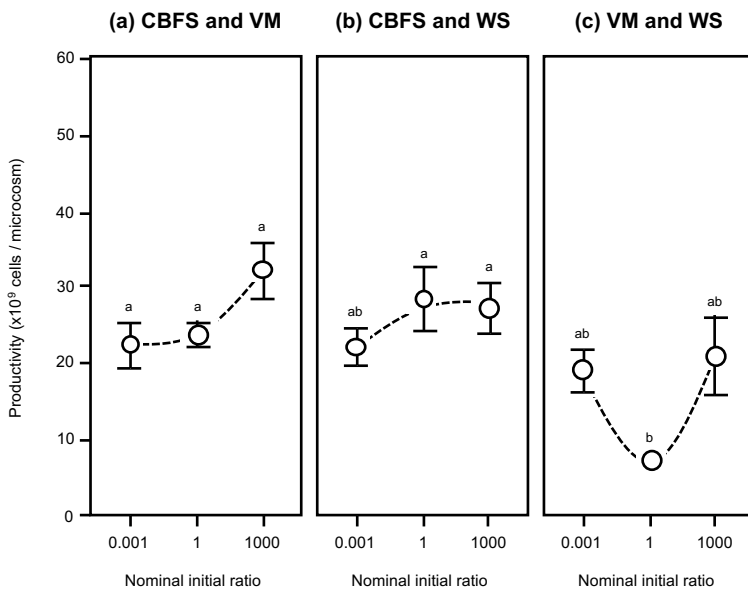


**Figure S4. Productivity in the pairwise competition assays.** Shown are the productivities determined as the total final cell numbers (a – c, CBFS and VM, CBFS and WS, and VM and WS) per microcosm for the competitive fitness assays with nominal initial cell ratios of 0.001, 1 and 1000. Means  $\pm$  SE ( $n = 5$ ) are shown. Means not connected by the same letter within and across panels are significantly different (T-K HSD,  $\alpha = 0.05$ ). Dashed lines indicate trends only.